MARYLAND

TECHNICAL RESEARCH REPORT

SRC TR 88-105

Synthesis and Analysis of Geared Robotic Mechanisms

by

S.-L. Chang and L.-W. Tsai

SYSTEMS RESEARCH CENTER

UNIVERSITY OF MARYLAND

COLLEGE PARK, MARYLAND 20742

Synthesis and Analysis of Geared Robotic Mechanisms

Sun-Lai Chang

Graduate Research Assistant

Lung-Wen Tsai

Associate Professor

Member of ASME

Mechanical Engineering Department

and

Systems Research Center

University of Maryland

College Park, MD 20742

This work has been supported in part by the U.S. Department of Energy, Grant No. DE-FG05-88ER13977 and in part by NSF Engineering Research Centers Program, NSFD CDR 8803012. Such supports do not constitute an endorsement by the supporting agencies of the views expressed in the article.

Abstract

In this paper we introduce the concept of transmission lines for kinematic analysis and synthesis of geared robotic mechanisms. It is shown that the structural matrix, which relates input displacements to the joint angles of a multi-degree-of-freedom geared robotic mechanism, can be derived using the concept of transmission lines. Applying the characteristics of structural matrix, a new methodology for structural synthesis of articulated mechanisms has been established. All the basic admissible structural matrices of three-degree-of-freedom robotic mechanisms have been enumerated to demonstrate the principle. Several arm and wrist mechanisms created are believed to be new and novel.

1. Introduction

The kinematic structure of a robotic mechanism often takes the form of an open-loop configuration. An open-loop manipulator is mechanically simple and easy to construct. However, it does require the actuators to be located along the joint axes which, in turn, increases the inertia of the manipulator. For this reason cable and push/pull elements are commonly used to permit the actuators to be located at the base or as close to the base as possible (Morecki, et al. 1980; Salibury, 1982). However, cable-driven robot manipulators do suffer the problem of limited payload and large vibrations. To overcome this difficulty, recently Tsai and Freudenstein (1988) investigated the kinematic structure of relatively small robots with positive, rigid-body drive elements. Several novel robot configurations were conceived. However, the design alternatives suggested by Tsai and Freudenstein are representative rather than exhaustive. In the light of these considerations, we have developed a more efficient methodology for the structural synthesis of geared robotic mechanisms.

The structural synthesis of geared mechanisms has been accomplished by graph theorem in recent years (Buchsbaum and Freudenstein, 1970; Freudenstein, 1971; Freudenstein and Maki, 1979; and Tsai, 1987a). Using graph representation, the function of a desired mechanism is separated from structural consideration during the initial conceptual design stage. First, kinematic structures of the same type, i.e. same number of links, degrees of freedom, etc., are enumerated systematically. Then potentially useful mechanism structures are selected for the purpose of functional evaluation. The method of graph representation is very thorough and systematic.

However, when the number of links increases, it becomes very complicated and difficult to deal with. In this paper we introduce a new method of structural synthesis. This new method allows us to perform the synthesis of geared robotic mechanisms from both structural and functional points of view.

2. Structural Representations

Various methods have been used to represent the kinematic structure of a mechanism. In what follows, we shall review a few that are pertinent to the development of this paper.

(a) Functional Representation. This refers to the conventional drawing of a mechanism. Shafts, gears and other elements are identified as such. For the reason of clarity and simplicity, only functional elements essential to the kinematic structure are shown. Different functional representations may represent different designs of the same topological structure (e.g. planar vs. spatial mechanisms, internal gear mesh vs. external gear mesh).

For example, the functional representation of the Cincinnati Milacron T^3 wrist is shown in Fig. 1(a), where three bevel gear pairs, 6-2, 3-5 and 4-5, transmit power to the end-effector through three articulated joint axes, Z_1, Z_2 and Z_3. We note that, in addition to the gear dimensions, the geometry of this mechanism can be defined by the Hartenberg and Denavit parameters, i.e. the offset distance, twist angle and translational distance between two adjacent axes (Hartenberg and Denavit, 1964).

(b) Planar Representation. In this representation, a positive direction of rotation is assigned to each joint axis in the mechanism of interest. Then,

starting from the second joint axis, every axis is twisted about the common normal defined by the axis itself and its preceding axis until all the joint axes are parallel to each other and are pointed toward the same positive Z-direction. Finally, all the bevel gears are replaced by spur gears and if two adjacent axes intersect at a point, then an offset distance is added to permit the spatial bevel gears to be replaced by equivalent planar spur gears. The gear mesh, internal or external, depends on whether a positive rotation of one gear with respect to its positive joint axis results in a positive or negative rotation of the mating gear. Figure 1(b) shows the planar representation of Fig. 1(a). For the reason of simplicity, sometimes all the gear meshes will be represented by external gear mesh only. The simplified planar representation of the Cincinnati Milacron T^3 wrist is shown in Fig. 1(c).

3. The Kinematics of Robotic Mechanisms

The kinematic analysis of geared robotic mechanisms can be easily accomplished by applying the concept of equivalent open-loop chain and the theory of fundamental circuits (Tsai, 1987b). Generally, the number of articulation points in a robotic mechanism is equal to the number of DOF (degree-of-freedom) and we shall assume that this is the case for the study to follow. Hence, the number of joints in the equivalent open-loop chain is also equal to the number of DOF.

According to Tsai's approach, the analysis of spatial robotic mechanisms can be divided into two steps. The first step is to derive the relationship between the position and/or orientation of the end effector and the joint

angles in the equivalent open-loop chain. The second step is to derive the relationship between the joint angles and the input displacements. The first step can be accomplished by the matrix method or the vector approach while the second step can be accomplished by applying the fundamental circuit equations and the coaxiality conditions (Tsai, 1987b).

For example, the Cincinnati Milacron T^3 wrist shown in Fig. 1(a) has an equivalent open-loop chain shown in Fig. 2, where a_k, α_k and d_k (k=1,2,3) are the Hartenberg and Denavit parameters. The relation between the joint angles and the end effector position and orientation can be written as (Tsai, 1987b):

$$\bar{P}_0 = T\,\bar{P}_3 \tag{1}$$

and

$$\bar{U}_0 = T\,\bar{U}_3 \tag{2}$$

where T is the transformation matrix relating the coordinate in the 3^{rd} coordinate system to that in the 0^{th} coordinate system and is a function of the Hartenberg and Denavit parameters, $\bar{P}_i$ is the position vector of a point in the end effector and expressed in the i^{th} coordinate system, and $\bar{U}_i$ is a unit vector attached to the end effector and expressed in the i^{th} coordinate system.

The fundamental circuit equations are given by:

$$\theta_{32} = -N_{53}\,\theta_{52} \tag{3}$$

$$\theta_{41} = -N_{54}\,\theta_{51} \tag{4}$$

$$\theta_{61} = N_{26}\,\theta_{21} \tag{5}$$

And the coaxiality conditions are:

$$\theta_{52} = \theta_{51} - \theta_{21} \tag{6}$$

$$\theta_{41} = \theta_{40} - \theta_{10} \tag{7}$$

$$\theta_{61} = \theta_{60} - \theta_{10} \tag{8}$$

where θ_{ij} denotes the relative angular displacement of link i with respect to link j, and $N_{jk} = N_j/N_k$ is the gear ratio of gears j and k with N_j and N_k teeth, respectively.

Solving eqs. (3) to (8), we obtain

$$\theta_{40} = \theta_{10} - N_{54}\,\theta_{21} + N_{35}\,N_{54}\,\theta_{32} \tag{9}$$

$$\theta_{60} = \theta_{10} + N_{26}\,\theta_{21} \tag{10}$$

$$\theta_{10} = \theta_{10} \tag{11}$$

Writing eqs. (9)-(11) in matrix form, we obtain:

$$\bar{\phi} = B\,\bar{\theta} \tag{12}$$

where

$$B = \begin{bmatrix} 1 & -N_{54} & N_{35}N_{54} \\ 1 & N_{26} & 0 \\ 1 & 0 & 0 \end{bmatrix},$$

$\bar{\phi} = [\,\phi_1\,,\,\phi_2\,,\,\phi_3\,]^T = [\theta_{40}\,,\,\theta_{60}\,,\,\theta_{10}\,]^T$ = input displacements, and

$\bar{\theta} = [\,\theta_{10},\,\theta_{21},\,\theta_{32}\,]^T$ = joint angles

where $[\ ]^T$ denotes the transpose of $[\ ]$.

It can be shown that the equation relating the joint torques to the input torques is given by:

$$\bar{\tau} = B^T \bar{m} = A \bar{m} \tag{13}$$

where $\bar{\tau} = [\tau_1, \tau_2, \tau_3]^T$ denotes the resultant torques about joint axes 1, 2 and 3, and $\bar{m} = [m_1, m_2, m_3]^T$ denotes the input torques applied at links 4, 6, and 1, respectively. The matrix A, the transpose of B, is determined by the structural topology of the mechanism and the gear ratios. We call the matrix A, the structural matrix of the mechanism.

4. Transmission Lines

Taking the derivative of eq. (13), we obtain:

$$d\bar{\tau} = A \, (d \, \bar{m}) \tag{14}$$

Hence, the (i,j) element of matrix A can be interpreted as the partial rate of change of the joint torque, τ_i, with respect to the input torque, m_j, i.e.

$$a_{ij} = \partial \tau_i \, / \, \partial m_j \tag{15}$$

Hence, $a_{ij} \neq 0$ implies that torque m_j will be transmitted to joint i and amplified by a_{ij} times, and $a_{ij} = 0$ implies that input torque m_j doesn't have any influence on the resultant torque at joint i. Therefore, the i^{th} row of the structural matrix A describes how the resultant torque about joint i is effected by the input actuators and, on the other hand, the j^{th} column of matrix A describes how the torque of an input actuator j is transmitted to various joints of the mechanism. For the type of mechanisms considered, removal of all the gears from the mechanism results in an open-loop chain. Hence except for the case of a direct drive, torques can be transmitted by gear

trains only, and the joint torques affected by an actuator must be consecutive. The gear train which results in a series of non-zero elements in the k^{th} column is, therefore, called the transmission line for the input actuator k.

Figure 3 shows a typical transmission line in planar representation where a series of links, numbered i, i+1,..., i+j, are connected together by revolute joints to form an open-loop chain, and where gears k, k+1,..., k+j-1 are pivoted about the i^{th}, $(i+1)^{th}$,..., and $(i+j-1)^{th}$ joint axes, respectively. The last gear, (k+j-1), is attached to link (i+j), and the rotation of gear k with respect to link i is considered as the input.

For such a transmission line, the fundamental circuit equations can be written as follows:

$$\theta_{(m-1)n} = \pm N_{m(m-1)}\theta_{mn} \tag{16}$$

where

$$m = (k+1),(k+2),\ldots,(k+j-1)$$

$$n = m-k+i$$

and where the sign of eq. (16) depends on whether the gear mesh is internal or external.

The coaxiality conditions can be written as:

$$\theta_{mn} = \theta_{m(n+1)} + \theta_{(n+1)n} \tag{17}$$

where $m = k, k+1, \ldots k+j-2$

$$n = m - k + i$$

We note that $\theta_{k+j-1} = \theta_{i+j}$, since the last gear, (k+j-1), is attached to link (i+j). Using eqs. (16) and (17), we can prove that

$$\theta_{ki} = \sum_{n=1}^{j} b_{kn}\, \theta_{(i+n)(i+n-1)} \qquad (18)$$

where

$$b_{k1} = 1 \ ,$$

$$b_{kn} = \pm\, b_{k(n-1)}\, N_{(k+n-1)(k+n-2)}, \qquad n=2,3,\ldots,j$$

and, where the sign depends on the gear mesh between links (k+n-1) and (k+n-2). The angle θ_{ki} denotes the displacement of the input link, k, with respect to its reference link i, and the angles $\theta_{(i+n)(i+n-1)}$, n=2, 3,...,j, denote the joint angles of the open-loop chain in the transmission line.

Following eq. (18), we conclude that the coefficient b_{kn} is equal to the train value defined from the gear pivoted about the n^{th} joint axis to the input gear, k. For example, b_{13} for the Cincinnati Milacron T^3 wrist is equal to the train value defined from gear 3 pivoted about the 3^{rd} joint axis to the input gear 4, and is equal to $(+N_{35}\, N_{54})$, where the positive sign comes from the fact that when the input link makes a positive rotation with respect to Z_1-axis, gear 3 will also make a positive rotation with respect to Z_3-axis. Hence, the coefficient of the structural matrix, $a_{nk} = b_{kn}$, can be determined by writing eq. (18) as many times as the number of inputs. Note that if the stator of a motor is mounted on the i^{th} link and the rotor is connected to the $(i+1)^{th}$ link, and there are no other gears connected to the motor, then we have a direct drive. The coefficient of matrix for a direct drive is equal to one, i.e. $\theta_{ki} = \theta_{(i+1)i}$.

5. Methodology of Synthesis

As discussed in the previous section the joint torques of a geared robotic mechanism are related to the input torques by a linear transformation called the structural matrix. There exists a unique structural matrix corresponding to a given mechanism. On the other hand, given a structural matrix, we can construct either planar spur-gear, or spatial bevel-gear mechanisms. The creation of mechanisms can, therefore, be accomplished by the enumeration of structural matrices followed by the construction of mechanisms.

(a) Enumeration of Structural Matrices

For convenience of enumeration, we shall denote the non-zero elements of a structural matrix by the "#" sign and neglect the gear ratio and type of gear mesh temporarily. We shall consider only those n-DOF geared mechanisms with n articulation points. From the previous discussions, we conclude that the structural matrix, A, obeys the following rules:

(1) The matrix is an axn square matrix. Its determinant shall not be zero, otherwise the mechanism is uncontrollable.

(2) The matrix can always be arranged in a sequence such that the elements in the i^{th} row represent the influence coefficients for the i^{th} joint. We shall number the joint in sequence and define the one fixed to the reference frame as the first joint.

(3) Since the joints influenced by an actuator are consecutive, non-zero elements in a column of the structural matrix must also be consecutive, i.e., there can not exist one or more zero elements between any two non-zero elements in a column.

(4) Switching any two columns of the matrix results in a renumbering of the two corresponding actuators. Hence, two kinematic structures are

said to be isomorphic if their corresponding structural matrices become identical after repeated operations of column exchange.

Applying the above rules, structural matrices can be synthesized in a systematic manner. For example, all the structural matrices for three DOF geared mechanisms with three articulation points have been enumerated and listed in Table 1. In this table, the matrices are arranged according to the distribution of the actuators. It is assumed that each actuator is to be located on the joint axis nearest to the ground of the corresponding transmission line. The letters "g", "s" and "e" denote the location of the actuators are on the 1^{st}, 2^{nd} and 3^{rd} joint axes, respectively, which correspond to the ground, shoulder and elbow joints of a robot arm, and the power stands for the number of actuators to be installed on that joint axis.

(b) Construction of Mechanisms. Once the structural matrix has been enumerated, the corresponding mechanisms can be constructed as follows:

(1) Construction of transmission lines. A transmission line can be constructed for each column of a structural matrix. For example the transmission lines corresponding to the structural matrix g^2s-8 are sketched in Fig. 4(a). Note that there are n transmission lines corresponding to an nxn structural matrix. These transmission lines share a common open-loop chain. The common open-loop chain always starts from the base link and ends at the end-effector link. Spur gears are then added on to the open-loop chain according to the existence of non-zero elements in the corresponding column of the structural matrix. The first gear of the k^{th} transmission line is to be pivoted about the joint axis corresponding to the row number of

the first non-zero element in the k^{th} column and is considered as the input link. The last gear of the k^{th} transmission line is to be pivoted about the joint axis corresponding to the row number of the last non-zero element in the k^{th} column, and is to be attached to the link which pivots about the same joint axis and belongs to the far-end of the open-loop chain. In the g^2s-8 example, the first column is $(\# \# 0)^T$. Hence, the open-loop chain consists of links 0, 1, 2, and 3, where link 0 is the base link and link 3 is the end-effector link. The first gear is pivoted about the first joint axis and is considered to be the input link. The second, which is also the last gear, is pivoted about the second joint axis and is attached to link 2. For the purpose of convenience only external gear meshes are used.

(2) Construction of Planar Mechanisms. All the transmission lines constructed above can be combined, using the common open-loop chain, to form a planar mechanism. For example the three transmission lines shown in Fig. 4(a) have been combined into a planar mechanism shown in Fig. 4(b).

(3) Addition of idler gears. The mechanisms derived from the above two steps shall be called the basic mechanisms. In order to change the direction of rotation, to achieve greater gear reduction and/or to extend the center distance between two adjacent articulation points, idler gears may be added to the basic mechanisms. For example Fig. 5(a) shows a transmission line with two meshing gears, while Fig. 5(b) shows the addition of an idler gear, gear j. We shall call

those mechanisms with the addition of one or more idler gears the derived mechanisms as opposed to the basic mechanisms.

(4) Construction of spatial or spherical mechanisms. Spatial or spherical mechanisms can be constructed by replacing the spur gears with bevel gears and the parallel joint axes with intersecting or skew joint axes. Fig. 5(c) shows a spatial transmission line derived from the planar schematic shown in Fig. 5(b). We note that idler gears are required for the construction of two non-intersecting joint axes.

6. The Creation of 3R Robotic Mechanisms

(a) 3R Robot Arms.

All the structural matrices listed in Table 1 can be used to construct spatial 3R robot arms. For example, using the structural matrix g^2s-8, three transmission lines and its planar basic mechanism have been sketched in Figs. 4(a) and 4(b) as discussed in the previous section. In order to convert the planar mechanism to a spatial one, we rearrange the joint axes such that the first two intersect perpendicularly, and the third is parallel to the second. Then, spur gears are replaced by bevel gears and, in addition, an idler gear is added to the third transmission line to accommodate for the large offset distance between the second and third joint axes. The resulting mechanism is shown in Fig. 6.

The transformation between input displacements and the joint angles for the 3R-arm shown in Fig. 6 can be obtained by writing eq. (18) three times, once for each transmission line,

$$\theta_{40} = \theta_{10} + N_{24}\,\theta_{21} \tag{19}$$

$$\theta_{10} = \theta_{10} \tag{20}$$

$$\theta_{51} = \theta_{21} - N_{36}\,N_{65}\,\theta_{32} \tag{21}$$

Writing eqs. (19)-(21) in matrix form, we obtain:

$$\begin{bmatrix} \theta_{40} \\ \theta_{10} \\ \theta_{51} \end{bmatrix} = \begin{bmatrix} 1 & N_{24} & 0 \\ 1 & 0 & 0 \\ 0 & 1 & -N_{36}\,N_{65} \end{bmatrix} \begin{bmatrix} \theta_{10} \\ \theta_{21} \\ \theta_{32} \end{bmatrix} \tag{22}$$

Hence, the structural matrix is:

$$A = \begin{bmatrix} 1 & 1 & 0 \\ N_{24} & 0 & 1 \\ 0 & 0 & -N_{36}\,N_{65} \end{bmatrix} \tag{23}$$

which is in complete agreement with the g^2s-8 matrix given Table 1.

In a similar manner, 3R robot arms can be constructed for each of the structural matrices listed in Table 1. We note that the g^3 family permits all the motors to be ground connected, the g^2s family permits two motors to be ground connected and the third on the shoulder joint, the g^2e family permits two motors to be ground connected and the third on the elbow joint, the gs^2 family permits only one motor to be ground connected and the remaining two on the shoulder joint, and lastly, the gse family requires the motors to be distributed one on each joint axis. The selection of the type of family is a compromise between mechanical complexity, inertia load and the coupling, and is not the subject of this investigation. However, suggestion can be made for

the selection of designs among the structural matrices within each family. From mechanical complexity and coupling points of view, we believe the g^3-5, g^2s-7 and g^2s-8, g^2e-5, gs^2-6, and gse-6 are the least complex and least coupled structure matrices for the g^3, g^2s, g^2e, gs^2 and gse families, respectively. For this reason, a 3R arm corresponding to each of the aforementioned structural matrices has been constructed and listed in Table 2. The joint axes for each of the 3R arms listed in Table 2 have been arranged in a configuration similar to that of the PUMA arm. We note that the mechanism configurations g^3-5 and gs^2-6 shown in Table 2 were recently revealed by Tsai and Freudenstein (1988).

(b) 3R Wrists

In practice, in order to reduce the inertia load of a manipulator, the wrist design must be compact and light weight. The actuators of a wrist mechanism are generally located on the base link of the wrist. The g^3 family listed in Table 1 permits all the actuators to be located on the base and are recommended for the wrist design. For the purpose of demonstration, the mechanism corresponding to the structural matrix g^3-5 is constructed as an example. Three transmission lines constructed according to the structural matrix g^3-5 are shown in Fig. 7(a). The combination of these three transmission lines into a planar mechanism is shown in Fig. 7(b). After the three joint axes are made to intersect at a point and the spur gears are replaced with bevel gears, we obtain a spherical wrist mechanism as shown in Fig. 7(c). Note that this mechanism structure is identical to that of the Cincinnati Milacron T^3 wrist (Stackhouse, 1979).

As noted earlier, idler gears can be added to modify the gear ratio or to change the direction of rotation. Figure 7(d) shows the addition of an idler gear 7 between the gear mesh 3-5 of the mechanism shown in Fig. 7(c). We note that this becomes the structure of PUMA wrist.

Following the same procedure, all the recommended basic spherical wrist mechanisms have been constructed and listed in Table 3. It is interesting to note that the g^3-3 mechanism is structurally the same as the Bendix wrist (Anonymous, 1982).

7. Summary

The concept of transmission lines has been introduced for the kinematic analysis of geared robotic mechanisms. Using the concept, a set of rules for the enumeration of structural matrices has been derived, and a procedure for the construction of basic mechanisms, planar or spatial, has been developed. it is also shown that idler gears can be added to these basic mechanisms to form additional mechanisms.

We believe this method of enumeration is more straightforward and more efficient than that of graph representation. The design can be started from a desired structural matrix, i.e. a desired mechanical coupling, instead of searching for all the admissible mechanisms as is the case of graph theorem. The theorem has been demonstrated by the enumeration of three DOF robotic arms and wrists. Some of the mechanism configurations presented are believed to be new and novel, and deserve further studies.

References:

Anonymous, August 1982, "Bevel Gear Make Robot's "Wrist" More Flexible," Machine Design, Vol. 54, No. 18, pp. 55.

Buchsbaum, F., and Freudenstein, F., 1970, "Synthesis of Kinematic Structure of Geared Kinematic Chains and Other Mechanisms," J. of Mechanisms and Machine Theory, Vol. 5, pp. 357-392.

Freudenstein, F., Feb. 1971, "An Application of Boolean Algebra to the Motion of Epicyclic Drives," ASME J. of Engineering for Industry, Vol. 93, Series B, pp. 176-182.

Freudenstein, F., and Maki, E.R., 1979, "The Creation of Mechanisms According to Kinematic Structure and Function," The International Journal of Architecture and Design, Environment, and Planning, Vol. 6, pp. 375-391.

Hartenberg, R.S., and Denavit, J., 1964, Kinematic Synthesis of Linkages, McGraw-Hill, New York.

Morecki, A., et al., March 1980, "Synthesis and Control of the Anthropomorphic Two-handed Manipulator," Proceedings of the 10th Inter. Symposium on Industrial Robots, Milan, Italy, pp. 461-474.

Salisbury, J.K., 1982, "Kinematic and Force Analysis of Articulated Hands," Ph.D. dissertation, Stanford University Dept. of Mechanical Engineering.

Stackhouse, T., 1979, "A New Concept in Wrist Flexibility," Proceedings of the 9th Int. Symposium on Industrial Robots, Washington, D.C., pp. 589-599.

Tsai, L.W., 1987a, "An Application of the Linkage Characteristic Polynomial to the Topological Synthesis of Epicyclic Gear Trains," ASME J. of Mechanisms, Transmissions, and Automation in Design, Vol. 109, No. 3, pp. 329-336.

Tsai, L.W., 1987b, "The Kinematics of Robotic Bevel-Gear Trains," Proceedings of the 1987 IEEE Inter. Conference on Robotics and Automation, Raleigh, N. Carolina: IEEE Journal of Robotics and Automation, Vol. 4, No. 2, April 1988.

Tsai, L.W., and Freudenstein, F., 1988, "On the Conceptual Design of a Novel Class of Robot Configuration," Accepted for publication in the ASME J. of Mechanisms, Transmissions, and Automation in Design, presented at the 1988 ASME Design Technology Conferences, Trends and Developments in Mechanisms, Machines and Robotics, DE-Vol. 15-3, Sept. 25-28, 1988, pp. 193-200.

Figure and Table Caption:

Fig. 1(a): Functional Representation of the Cincinnati Milacron T^3 wrist.

Fig. 1(b): The Planar Representation of Fig. 1(a).

Fig. 1(c): The Simplified Planar Representation of Fig. 1(a).

Fig. 2: The Equivalent Open-Loop Chain of Cincinnati Milicron T^3 wrist.

Fig. 3: A Typical Transmission Line.

Fig. 4(a): Three Transmission Lines Constructed According the g^2s-8 Matrix.

Fig. 4(b): The Combination of Three Transmission Lines into a Planar Mechanism.

Fig. 5(a): A Basic Transmission Line.

Fig. 5(b): The Addition of an Idler Gear.

Fig. 5(c): The Spatial Constructure of Fig. 5(b).

Fig. 6: A 3R Robot Arm Derived From Fig. 4(b).

Fig. 7(a): Three Transmission Lines Constructed According to the g^3-5 Matrix.

Fig. 7(b): The Combination of Three Transmission Lines into a Planar Mechanism.

Fig. 7(c): A 3-DOF Wrist Mechanism Derived From Fig. 7(b).

Fig. 7(d): A Wrist Mechanism With an Idler Gear Derived From Fig. 7(d).

Table 1: A List of Admissible 3R Structural Matrices.

Table 2: Some Recommended 3R Robot Arms.

Table 3: A List of Basic Wrist Mechanisms.

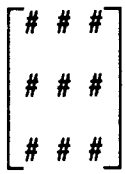

g^3-1

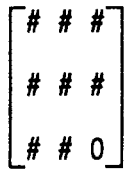

g^3-2

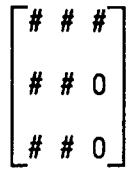

g^3-3

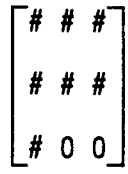

g^3-4

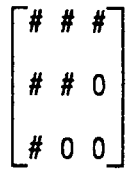

g^3-5

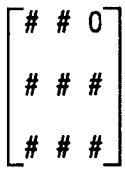

g^2s-1

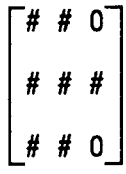

g^2s-2

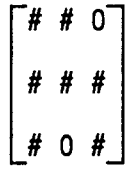

g^22-3

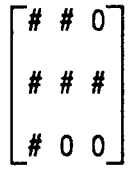

g^2s-4

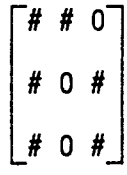

g^2s-5

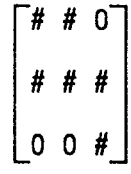

g^2s-6

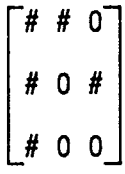

g^2s-7

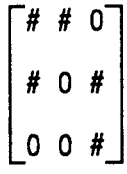

g^2s-8

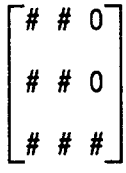

g^2e-1

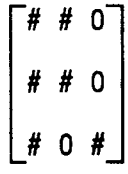

g^2e-2

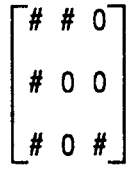

g^2e-3

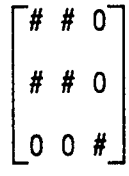

g^2e-4

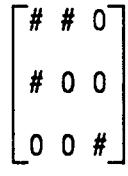

g^2e-5

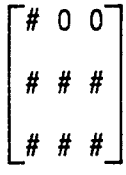

gs^2-1

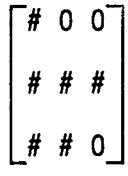

gs^2-2

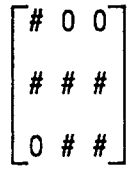

gs^2-3

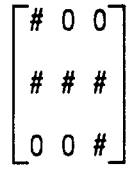

gs^2-4

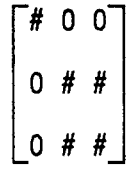

gs^2-5

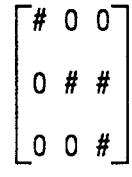

gs^2-6

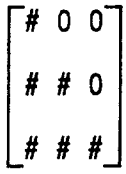

gse-1

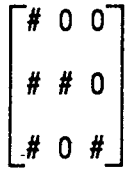

gse-2

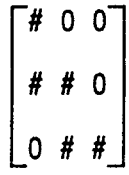

gse-3

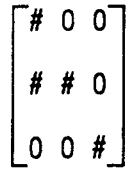

gse-4

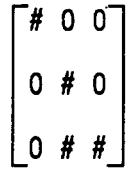

gse-5

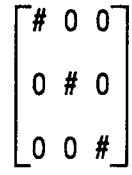

gse-6

Table 1

Table 2

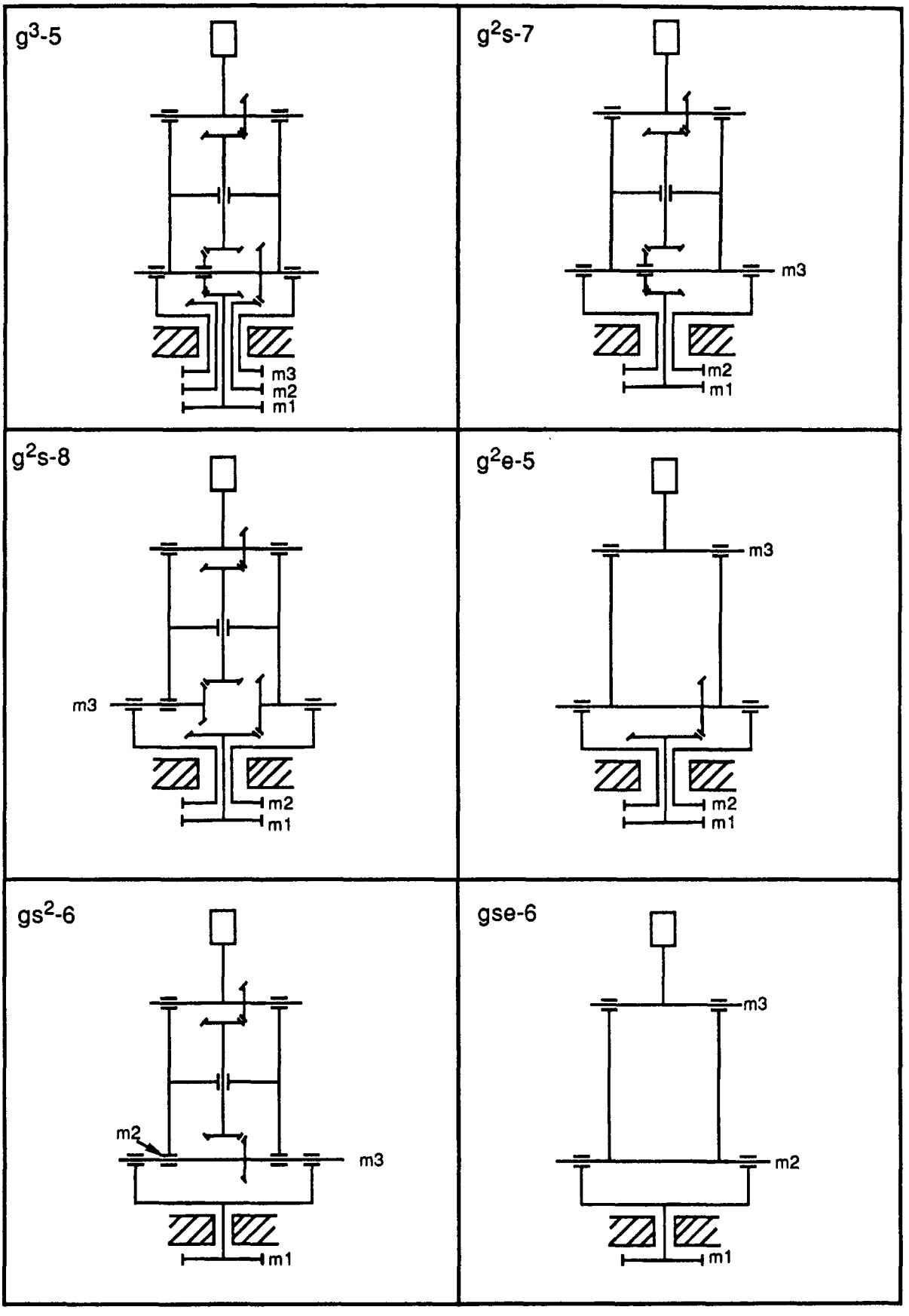

Note : The symbol "mk" denotes the k^{th} input.

Table 3

g^3-1

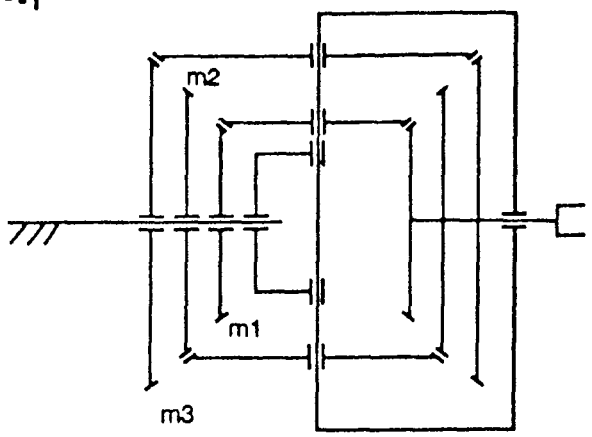

g^3-2

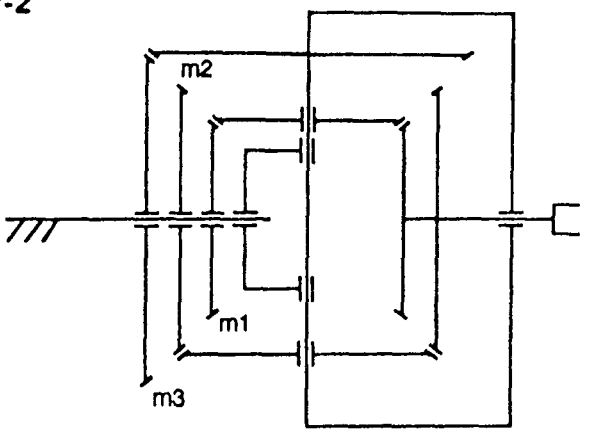

g^3-3

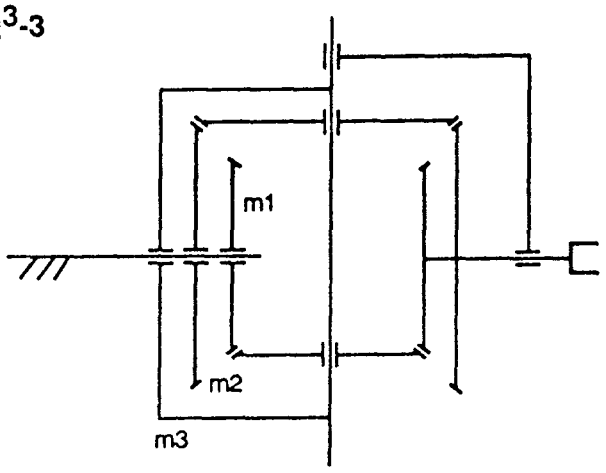

g^3-4

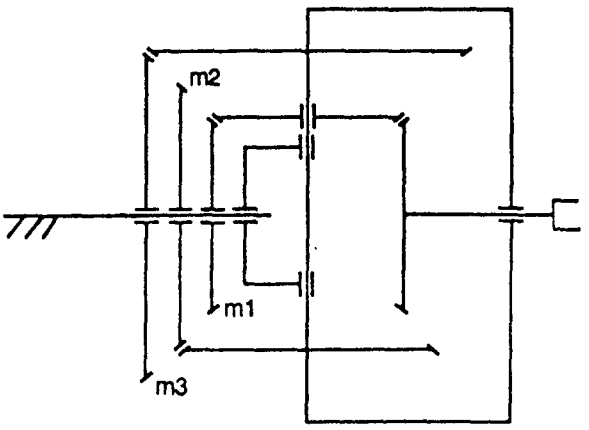

g^3-5

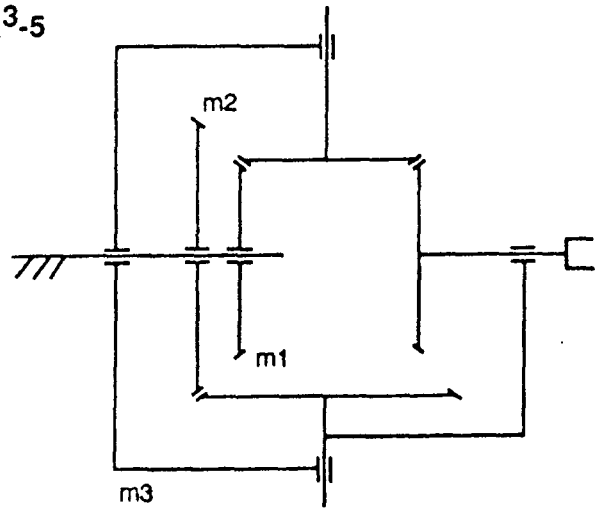

Note : The symbol "mk" denotes the k^{th} input.

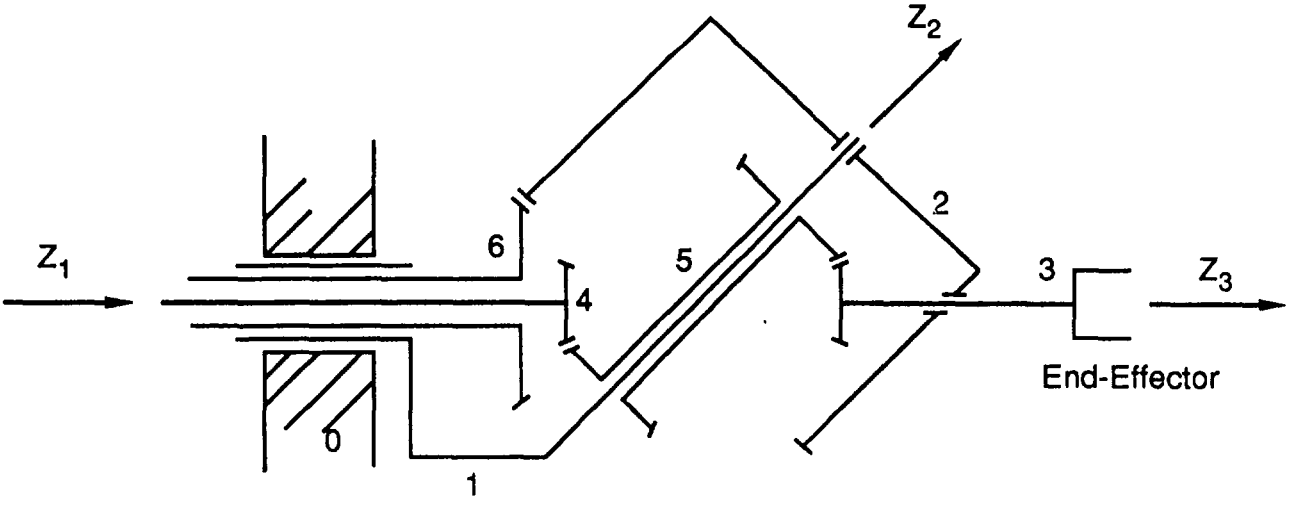

(a)

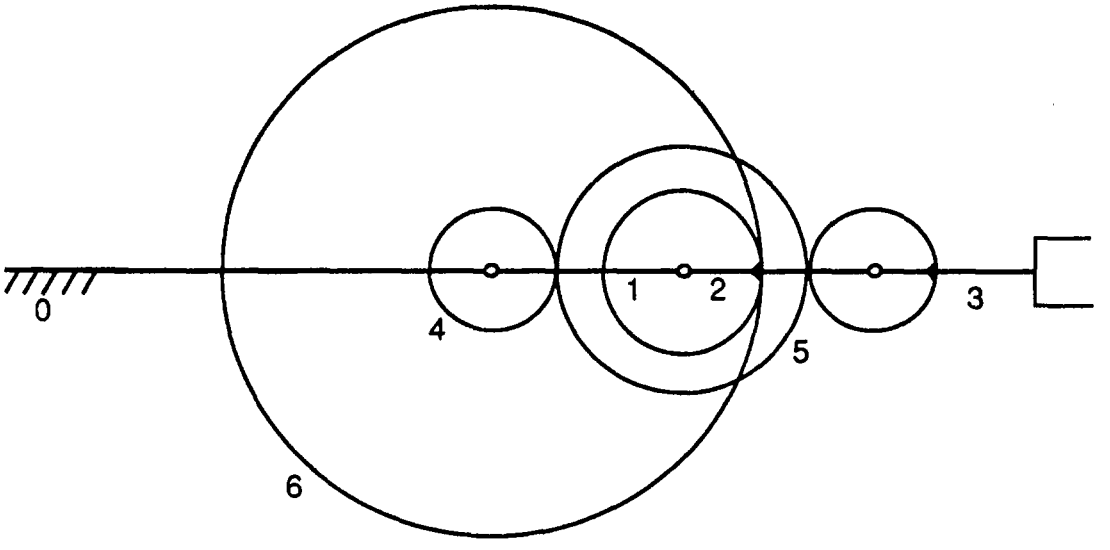

(b)

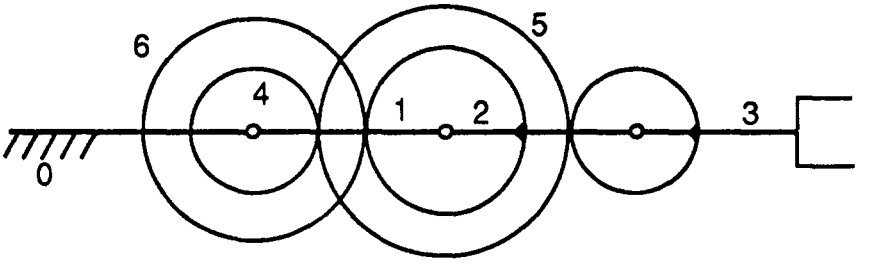

(c)

Fig. 1

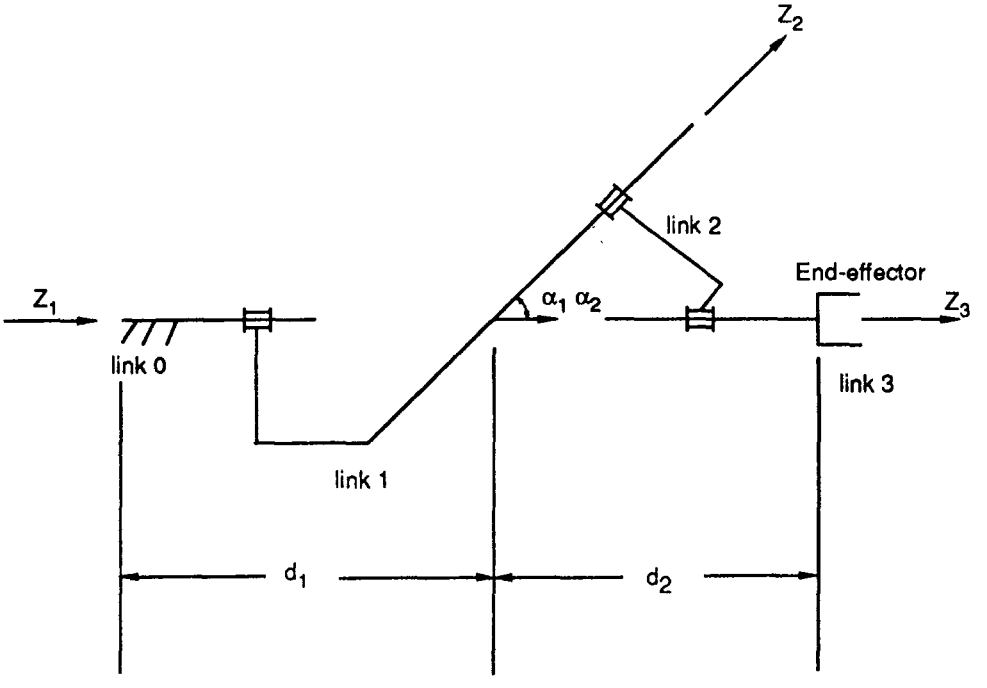
Z_2
link 2
End-effector
Z_1
α_1 α_2
Z_3
link 0
link 3
link 1
d_1
d_2

Fig. 2

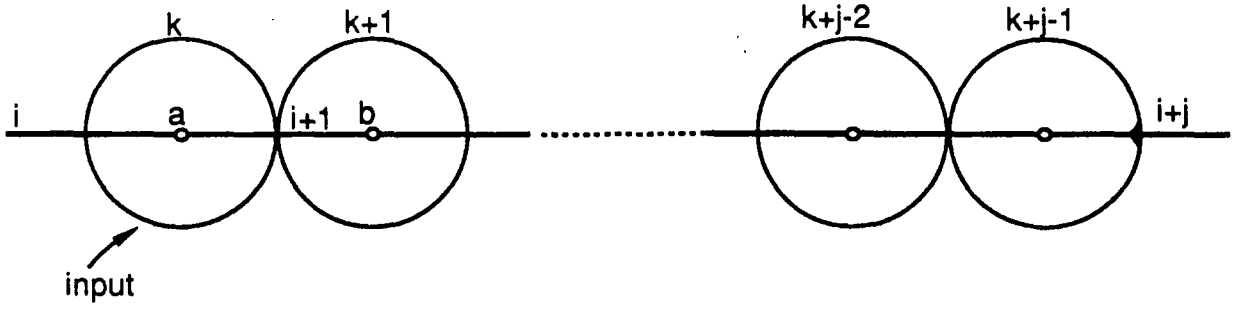

Fig 3

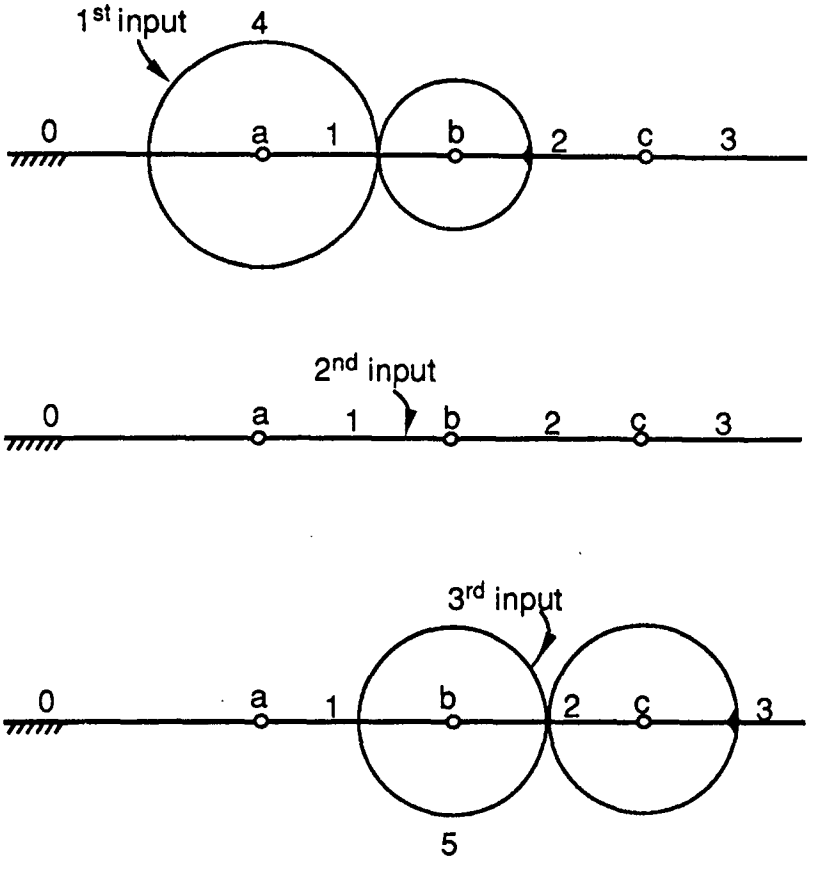
1st input
4
0
a
1
b
2
c
3
2nd input
0
a
1
b
2
c
3
3rd input
0
a
1
b
2
c
3
5

(a)

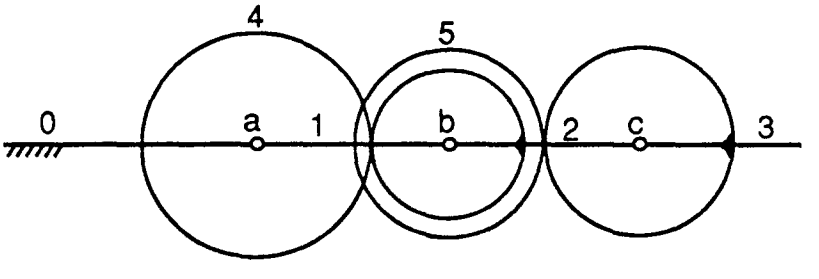
4
5
0
a
1
b
2
c
3

(b)

Fig. 4

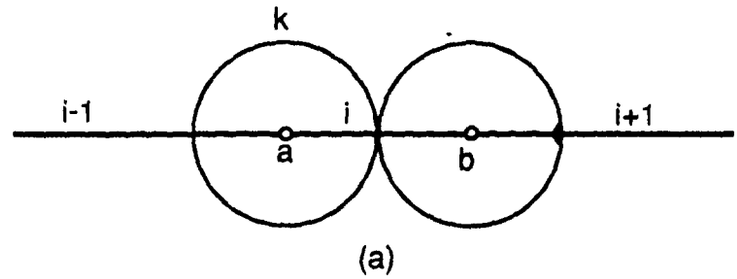

(a)

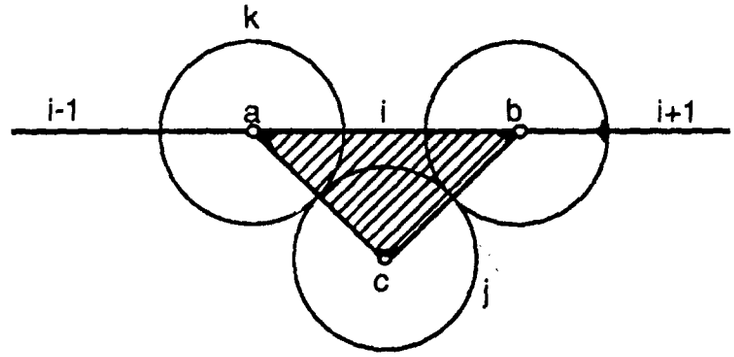

(b)

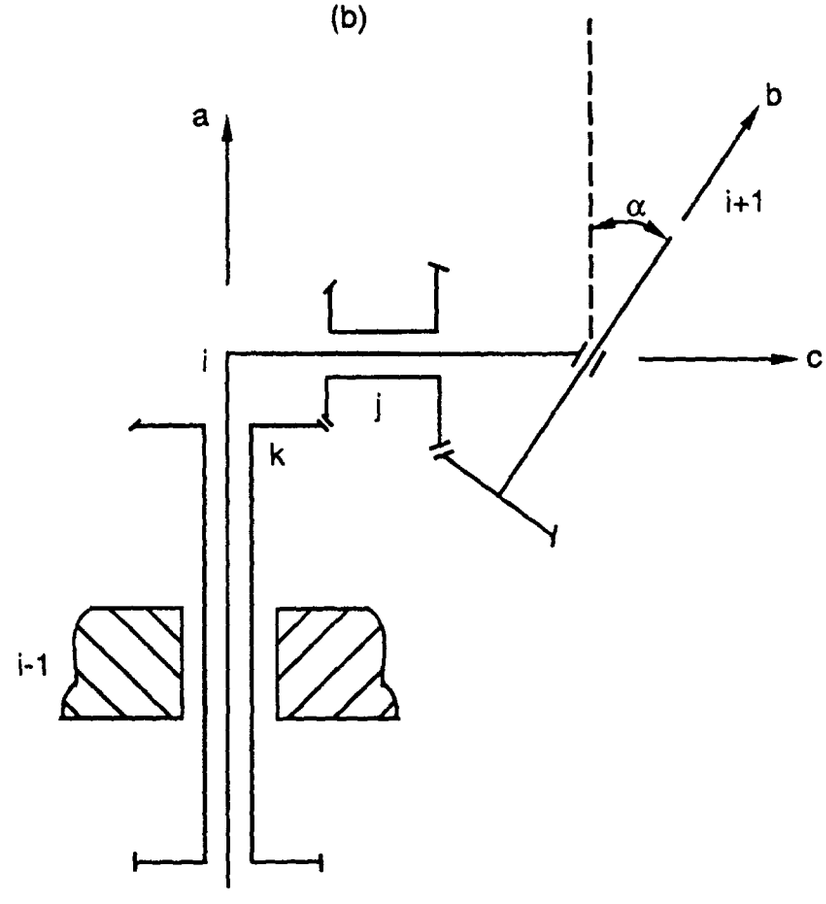

(c)

Fig. 5

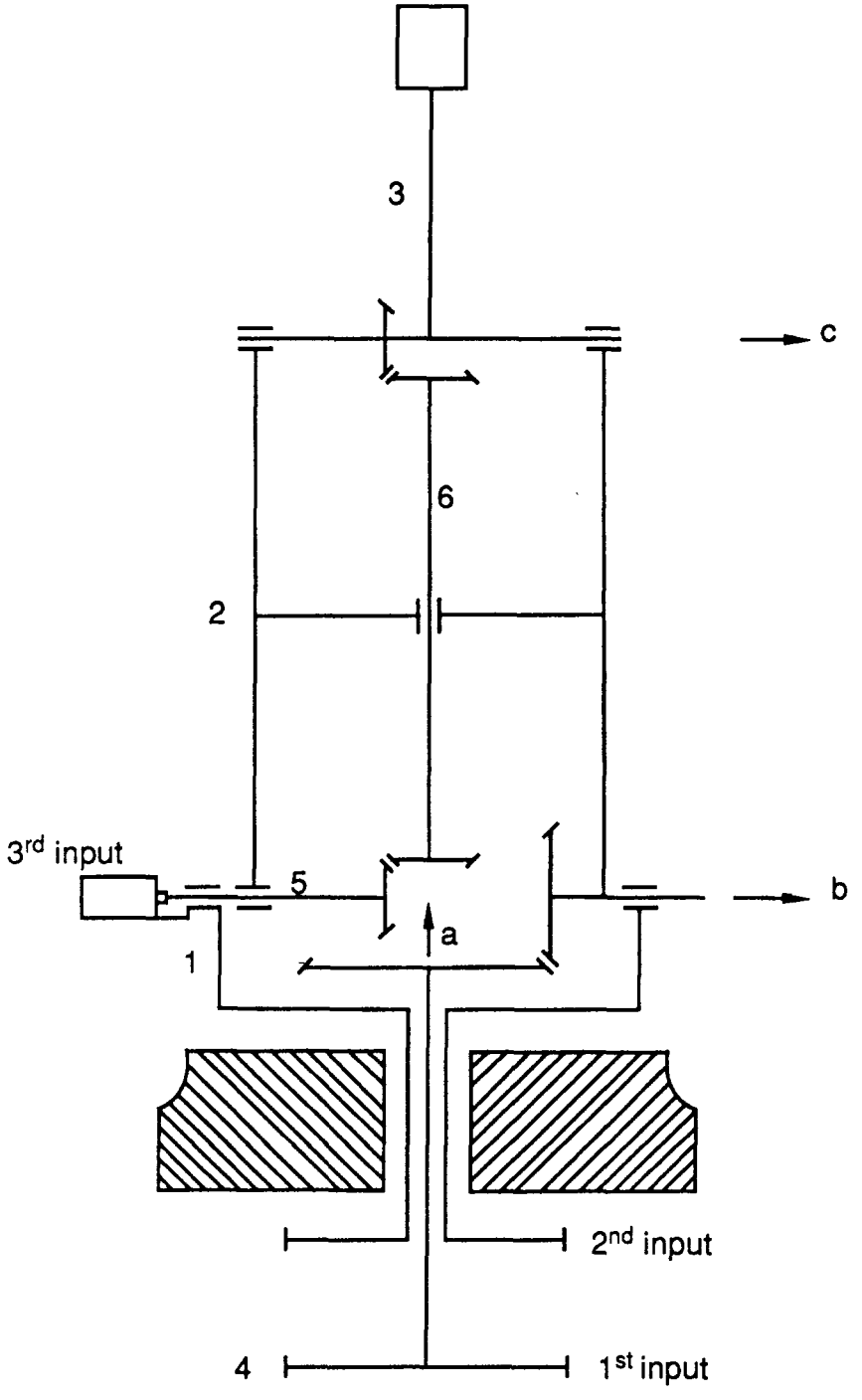

Fig. 6

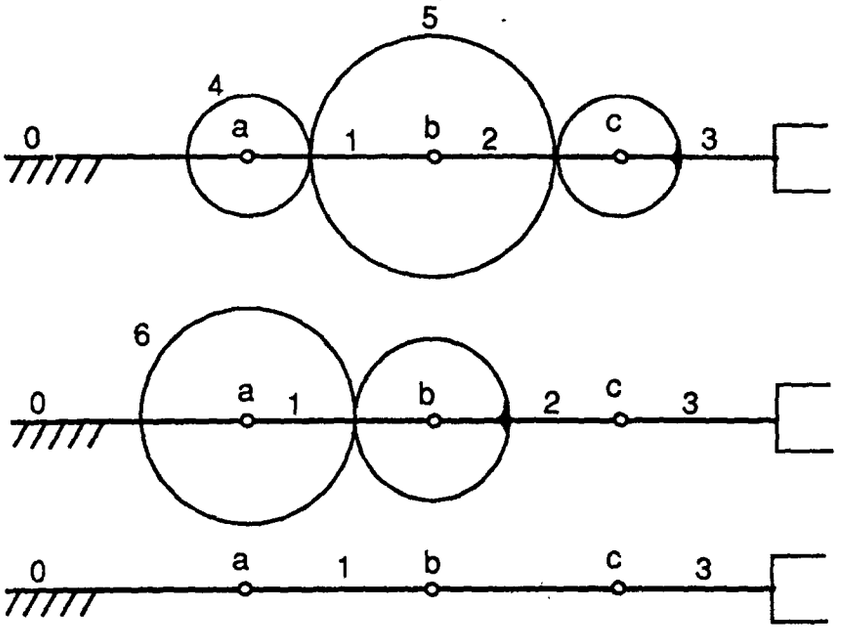

(a)

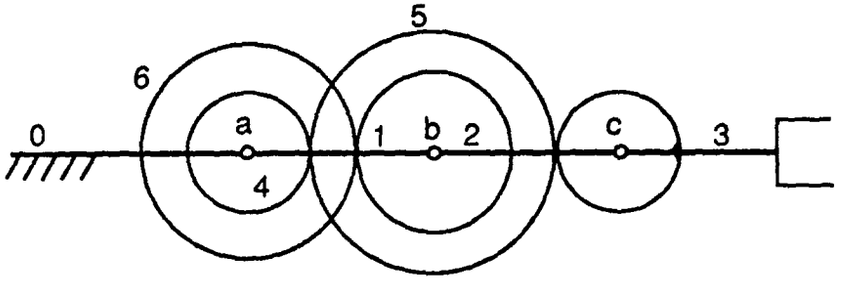

(b)

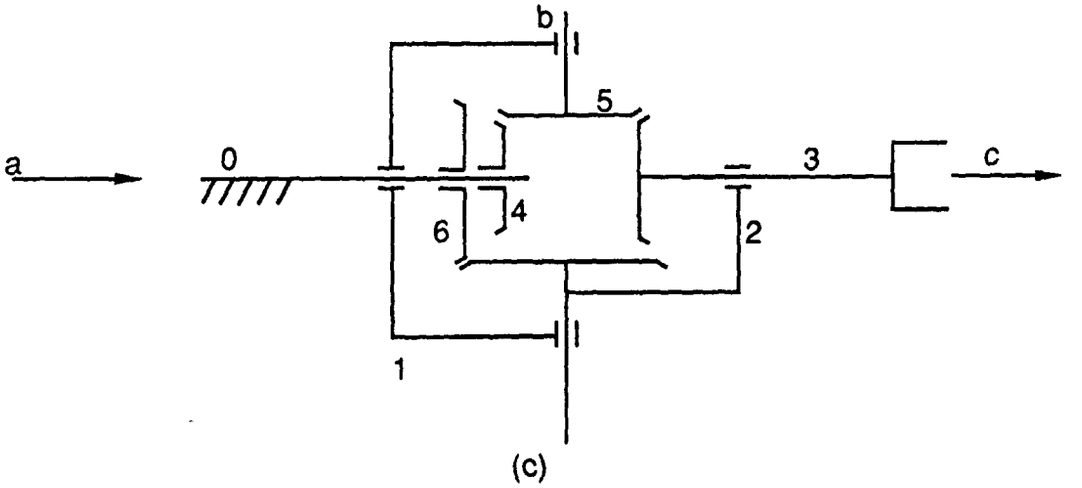

(c)

Fig. 7

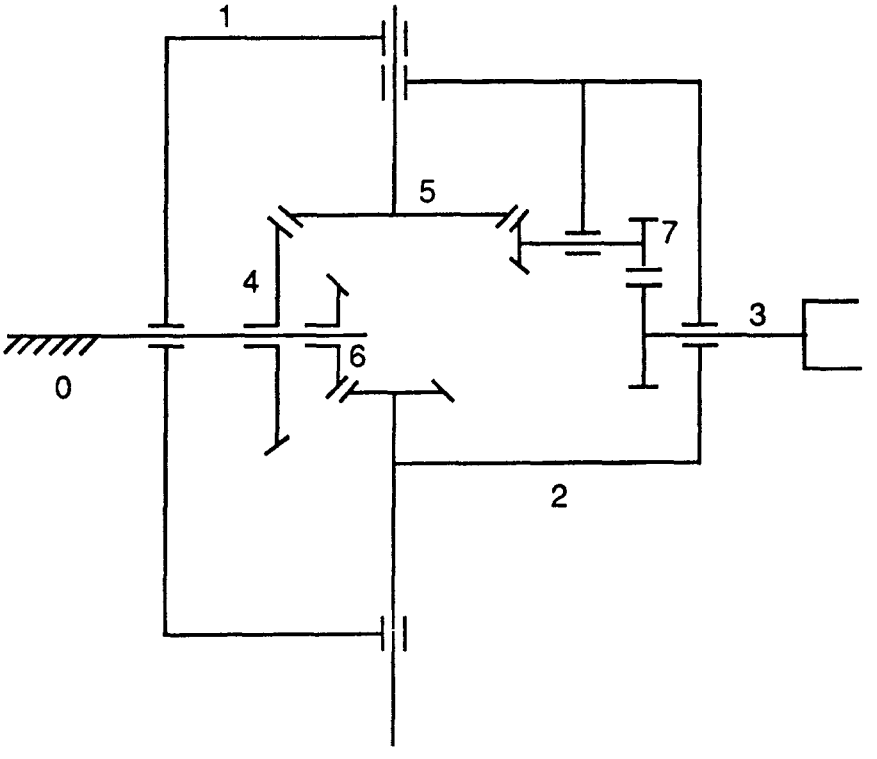

(d)

Fig. 7